



ANALYSIS OF DOWNHOLE DATA AND PRELIMINARY PRODUCTION CAPACITY ESTIMATE FOR THE OLKARIA DOMES GEOTHERMAL FIELD, KENYA

Joshua Niels Omenda Odeny
Kenya Electricity Generating Company,
Olkaria Geothermal Project,
P.O. Box 785, Naivasha,
KENYA

ABSTRACT

As a geothermal resource exploration strategy, the Kenya Electricity Generating Company carried out drilling of three deep wells in the Olkaria Domes geothermal field in 1998 and 1999. The Domes are located just to the southeast of the Olkaria East production field, which has been generating 45 MWe since 1986. The two fields, though physically separated by Ol Njorowa gorge, are within the boundaries of the greater Olkaria caldera. Systematic analysis of down-hole temperature and pressure profiles, injection, fall-off and discharge tests resulted in a conceptual reservoir model for the Domes. A permeable horizontal layer at 210-230°C temperature is identified between 1000 and 1400 m a.s.l. Fluid flow appears to be generally from north to south. Well transmissivities range between 0.4 and $3 \times 10^{-8} \text{ m}^3/\text{Pa s}$, which equals 1-6 mD permeability, assuming 500 m reservoir thickness. Injectivities range from 1.2 to 6.2 lps/bar. The conceptual reservoir model of the Domes is added to the greater Olkaria conceptual model. A dominating trend observed is that fluid drains naturally southwards and that the Domes area is peripheral to the main geothermal system. An energy reserve of 2-5 MWe is estimated for the Domes. A feasibility study suggests that the field is optimal for re-injection of up to 100 kg/s without substantial cooling of the nearby East production field.

1. INTRODUCTION

1.1 Location and general information

The Greater Olkaria geothermal area is situated southwest of Lake Naivasha in the eastern arm of the African Rift Valley in Kenya (Figure 1). It is divided into smaller fields namely East, Northeast, West, Central and Domes. The East field is fully developed with a 45 MWe power plant. The Northeast field is being developed for a 64 MWe power plant, while West and Central are being investigated for a possible binary power plant development (Muna, 1997). Many references on the Olkaria field development are available in the geothermal literature (Bödvarsson et al., 1987 and 1989; Haukwa, 1985).

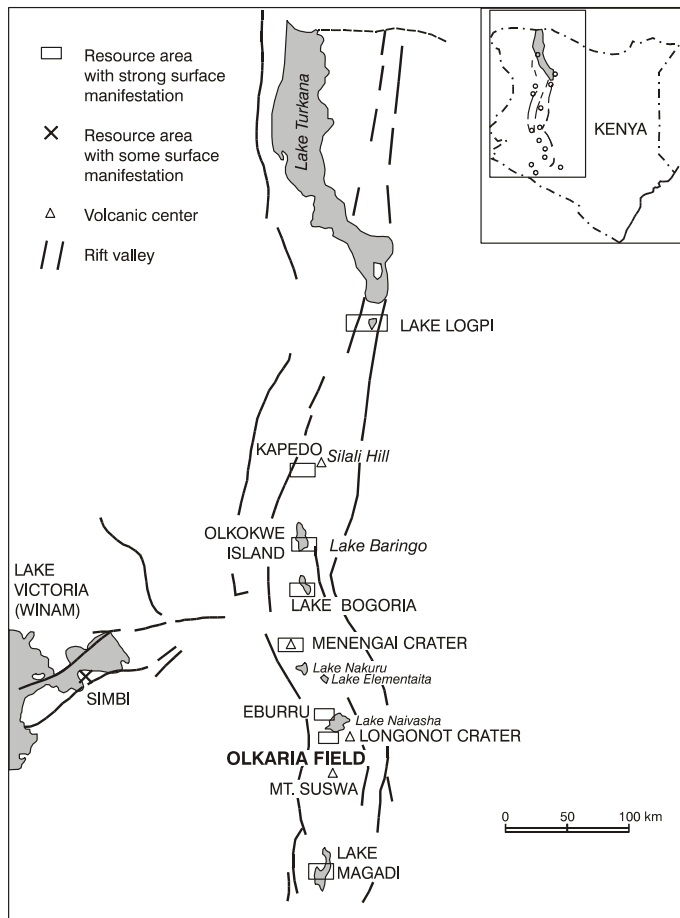


FIGURE 1: Location of the Olkaria geothermal field within the Rift Valley in Kenya

The Olkaria volcanic complex is one of several major volcanic centers situated in the Central Kenya Rift of the East African Rift system. These centers are associated with a N-S trending belt of peralkaline volcanism and substantial normal faulting. The rift valley floor is dominated by N-S and NNW-SSE trending faults and several NW-SE striking faults (Lagat, 1995). Most of the faults are attributed to evolution of the rift valley whereas some are attributed to local stresses due to underlying magma chambers.

The Olkaria Volcanic complex is thought to be a remnant of a caldera, cut by N-S normal rift faulting that provided loci for later eruptions of rhyolitic and pumice domes now exposed in the Ol Njorowa gorge (Figure 2). The surface is covered by ash falls from Mt Longonot and Mt Suswa and numerous comendite and palentellerite lavas. Areas of altered grounds, warm grounds and other surface manifestations of geothermal activity show a close association with the N-S structures, the ENE-WSW Olkaria fault zone and the ring domes. The rocks encountered downhole include pyroclastics, tuffs, rhyolites, trachites, phonolites, basalts and minor intrusives (Lagat 1995).

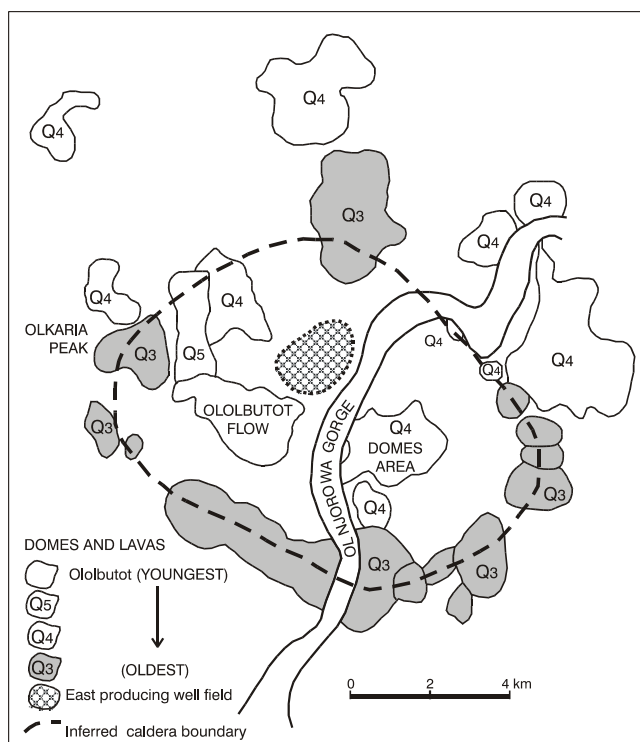


FIGURE 2: Olkaria caldera boundary, showing major domes and lavas (from Muna, 1997)

The Olkaria Domes field is at the southeastern end, within the ring structure that defines the greater Olkaria geothermal area, separated from the East field by Ol Njorowa gorge (Figure 2).

1.2 Scope of study

As a geothermal resource exploration strategy, the Kenya Electricity Generating Company carried out drilling of three deep wells in Olkaria Domes geothermal field. The wells are identified as OW-901, OW-902 and OW-903. They were drilled to completion between November 1998 and May 1999 and are still subjected to the various testing common after well completion. In this study, a conceptual model for the Olkaria Domes is constructed and analysed in terms of production capacity and feasibility of re-injection. Firstly, the results of down-hole temperature and pressure

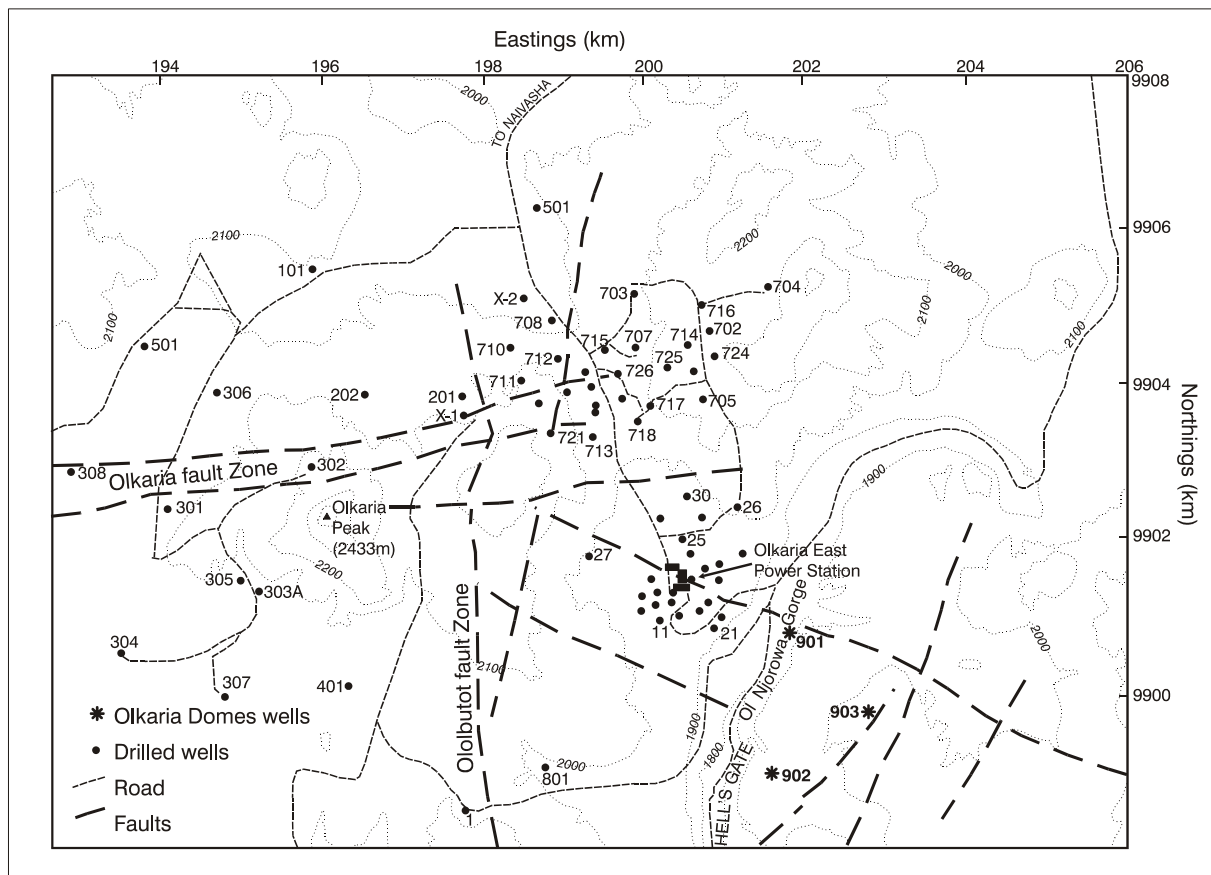


FIGURE 3: Location of wells in the greater Olkaria geothermal area; the Olkaria Domes wells are located in the SE sector of the map

logging, injection, fall-off and discharge tests are collected and interpreted in terms of initial reservoir pressure and formation temperature. Permeable zones are identified and transmissivity, permeability and injectivity are calculated. Using the available data, a preliminary conceptual model for the field is developed and this sub-model incorporated into the greater Olkaria geothermal area model. An estimate of the energy reserve and potential power output of the field is calculated, and feasibility of using the field for re-injection is also studied. This work should be regarded as preliminary, as more data will become available in the future. Furthermore, due to the strict time available, the work does not include other geosciences such as geology, geophysics and geochemistry.

Table 1 gives an overview of the Domes well locations and design. The physical location of the wells, relative to the greater Olkaria geothermal area, is shown in Figure 3.

TABLE 1: Location and description of wells in the Olkaria Domes

Well no.	Depth (m)	Eastings (m)	Northings (m)	Elevation (m a.s. l.)	9 5/8" casing shoe (m)	Top of 7" slotted liner (m)
OW-901	2199	201865	9900848	1890	758	729
OW-902	2201	201669	9898995	1957	648	624
OW-903	2205	202841	9899769	2043	697	670

2. WELL TESTING AND DATA SOURCES

2.1 Types of well tests

Various tests are usually carried out on geothermal wells to find the reservoir parameters which determine individual well and overall field performance. It is customary to isolate low temperature shallow feeds before the setting of production casing. Tests done on the upper part of a well during drilling are, therefore, usually designed to identify the formation static temperature and pressure profiles. Static formation pressure can be measured whenever loss of circulation occurs. However, measurement of actual static formation temperatures may involve halting of drilling operations, sometimes for more than one day. It is therefore advisable to use a combination of other methods to estimate the formation temperature. One such method is the study of cores and cuttings for alteration minerals. Analysis of warm-up temperature data may also become handy as is shown in Chapter 3.1 in this report.

The tests that are carried out at the completion of a well depend on the information required and the equipment available. In Olkaria, the tests done are transient pressure, injectivity, water loss and temperature and pressure profiles using Kuster/Amerada tools. In Iceland, for comparison, all these tests are done. In addition, neutron-neutron, natural gamma radiation, resistivity, caliper logs and differential temperature profiles are also commonly collected in Iceland.

After completion tests, the well is allowed to recover in temperature and pressure with regular monitoring. This is followed by a discharge test, to establish well output characteristics. Normally, the discharge test is followed by a shut-in test in which pressure is monitored for up to two or more months, in the shut-in well. But at the time of writing this report, this had not been done in Olkaria Domes. In fact, discharge tests were still continuing.

2.2 Completion tests and data sources

Completion tests in the Olkaria Domes wells were carried out using Kuster temperature and pressure gauges. The following format was applied:

1. Carrying out a combined downhole temperature and pressure survey immediately after landing the slotted liners to the well bottom.
2. Starting three-step injection tests by positioning the pressure tool just below the perceived feed zone and pumping water into the well. The pumping rates and duration were 16.7 kg/s for 3 hrs, 21.7 kg/s for 2¹/₂ hrs and 26.7 kg/s for 2¹/₂ hrs.
3. The tool was then retrieved while injection continued at 26.7 kg/s and a combined down-hole temperature and pressure survey was done.
4. The injection was stopped and pressure fall-off monitored for between 3 and 5 hours.
5. Down-hole temperature and pressure conditions were then routinely monitored over a period of time to identify the stable state of the wells.
6. The wells were then opened for discharge testing to estimate their production capacity.

The data for down-hole temperature and pressure surveys, injection and fall-off tests and preliminary discharge tests are now available. A total of forty eight down-hole pressure/temperature profiles have been collected, which amounts to 105 km of combined logging distance.

2.3 Discharge data

After a reasonable period of recovery, the Domes wells were put on discharge testing to determine their production capacities. Table 2 gives a summary of results obtained during these tests. It is evident from these results that all these wells are producing fluid of low enthalpy, at very low wellhead pressures. At this stage, we are, therefore, not able to obtain electric power with these pressures since they are lower than 5 Bar-a, which is the minimum required for conventional power generation.

TABLE 2: Summary of discharge tests results

Well no.	Duration (days)	Lip pipe diam. (mm)	WHP (bar-a)	Mass (kg/s)	Enthalpy (kJ/kg)	Water (kg/s)	Steam (kg/s)	Power (MW)
OW-901	1	203	4.45	21	1422	12	8	1.3
OW-901	5	127	5.97	10	1350	6	3	
OW-901	9	76	1.42	2	1580	1	1	
OW-901	4	102	4.94	8	1824	3	4	
OW-902	9	203	3.63	27	917	21	4	
OW-903	6	152	3.56	22	864	17	2	
OW-903	7	203	3.97	29	860	23	3	

3. ANALYSIS OF DOWNHOLE TEMPERATURE DATA

A temperature log is a set of temperature values recorded at different depths down a well. They provide important information on temperature conditions, flow paths and feed zones in geothermal systems. Temperature conditions are often affected by cooling during drilling, internal flow in shut-in wells and discharge in flowing ones. In this section, we analyse the logs obtained immediately after drilling, during injection tests and the recovery monitoring period in the Olkaria Domes geothermal field. Based on this analysis, a formation temperature profile is presented for all three wells.

3.1 Analysis of warm-up temperatures

Formation temperatures serve as a base for conceptual models of geothermal reservoirs and are important in making decisions upon well completion. However, due to cooling by circulation fluid during drilling, it is not possible to measure the formation temperature directly. Even if months or years have passed, boiling or convection may occur in the well making it impossible to probe the formation.

A computer software program, BERGHITI, has been developed at Orkustofnun, (Helgason, 1993). It is used for estimation of formation temperatures during recovery after drilling. It offers two methods of calculation; the Albright and the Horner methods.

The **Albright method** is used for direct determination of bottom-hole formation temperatures during economically acceptable interruptions in drilling operations. It assumes an arbitrary time interval, shorter than the total recovery time, and that the temperature relaxation depends only on the difference between the borehole temperature and the formation temperature. This method is commonly applied to warm-up time series shorter than 24 hours.

The **Horner method** is an analysis based on a straight line relationship between temperature, T and the logarithm of relative time, τ , where τ is given by

$$\tau = \frac{\Delta t}{\Delta t + t_0} \quad (1)$$

where Δt = The time passed since circulation stopped;
 t_0 = The circulation time.

It is evident that $\lim_{\Delta t \rightarrow \infty} \ln(\tau) = 0$. Using this and the fact that the system must have stabilised after infinite time, a plot of down-hole temperature as a function of $\ln(\tau)$ yields a straight line. Extrapolating the line to $\ln(\tau) = 0$, we are able to estimate the formation temperature. Note that this method is only valid for wells with no internal flow, thus it applies only to conductive warm-up. The Horner method was applied systematically to the down-hole temperature data collected so far from Olkaria Domes. Figure 4 presents an example of an excellent fit of the semi-log straight line relationship in well OW-902.

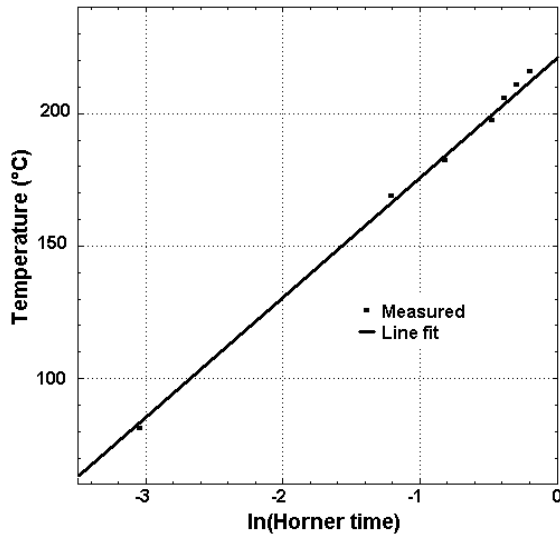


FIGURE 4: Formation temperature at 800 m depth in well OW-902

3.2 Downhole temperature conditions

In this section, all available temperature data in the Domes are plotted and analyzed in terms of formation temperature. Note that the Horner method is used extensively for all the wells. Numerical values of the formation temperature profiles are listed in Table 3.

Well 901: This well was completed on 20th November 1998 to a depth of 2212 m. Figure 5 shows a plot of all the available temperature profiles and the estimated formation temperature. The well temperature after drilling shows convective heating between 1500 and 900 m a.s.l. This suggests a possibility of shallow aquifers existing within this range. At 150 m a.s.l. there is a marked increase in the temperature gradient suggesting that most permeable zones are above this point. The temperature profile during injection indicates a slight gradient change between 700 and 600 m a.s.l., suggesting water loss into the formation and, hence, a feed-zone within these depths. Below 400 m a.s.l., the heating is very rapid suggesting that most of the cold water enters the formation above this point. The temperature profiles taken after fall-off also indicates a kick between 1400 and 900 m a.s.l., suggesting the existence of a hot feeder in this range. Subsequent recovery profiles taken after 12, 19, 27, 39, 60 and 83 days indicate higher recovery between 1400 and 300 m a.s.l. (average of 100°C from the pre-injection run), the highest being 122.5°C at 490 m a.s.l. The profile in this range is, however, conductive. This, together with the high temperature observed, suggests a heat source nearby.

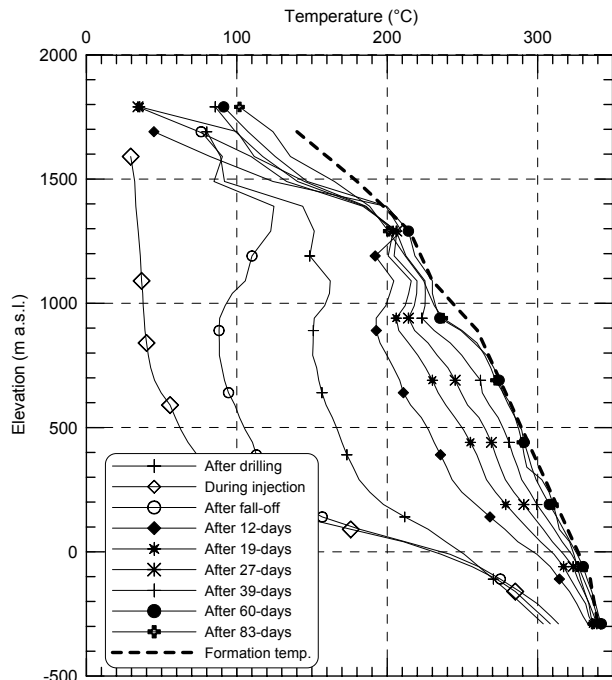


FIGURE 5: Temperature profiles in well OW-901

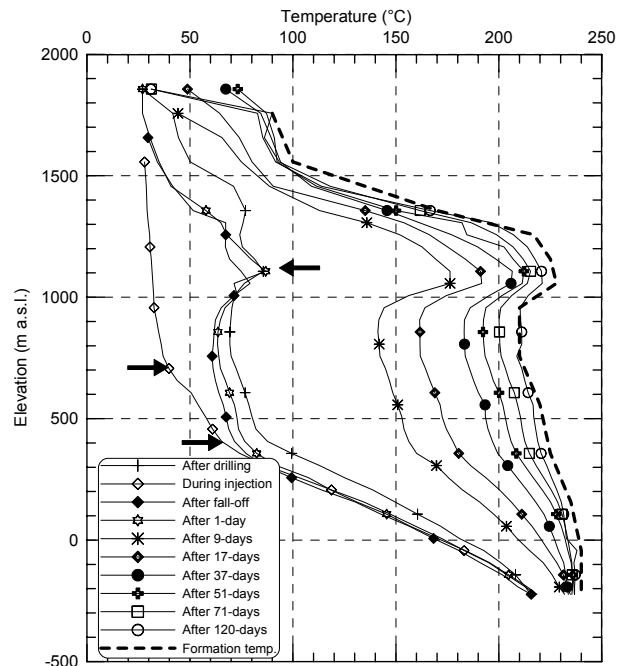


FIGURE 6: Temperature profiles in well OW-902; location of possible feed zones are shown by arrows

Well 902: Drilling of this well was completed on 14th February 1999. The down-hole temperature profiles and estimated formation temperature are shown in Figure 6. The pre-injection temperature profile shows convective heating between 1450 and 1050 m a.s.l., suggesting the possible existence of a shallow

aquifer. The temperature profiles taken after drilling show convective heating between 1500 and 900 m a.s.l. This suggests a possibility of shallow aquifers existing within this range. At 150 m a.s.l. there is a marked increase in the temperature gradient suggesting that most permeable zones are above this point. The temperature profile during injection indicates a slight gradient change between 700 and 600 m a.s.l., suggesting water loss into the formation and, hence, a feed-zone within these depths. Below 400 m a.s.l., the heating is very rapid suggesting that most of the cold water enters the formation above this point. The temperature profiles taken after fall-off also indicates a kick between 1400 and 900 m a.s.l., suggesting the existence of a hot feeder in this range. Subsequent recovery profiles taken after 12, 19, 27, 39, 60 and 83 days indicate higher recovery between 1400 and 300 m a.s.l. (average of 100°C from the pre-injection run), the highest being 122.5°C at 490 m a.s.l. The profile in this range is, however, conductive. This, together with the high temperature observed, suggests a heat source nearby.

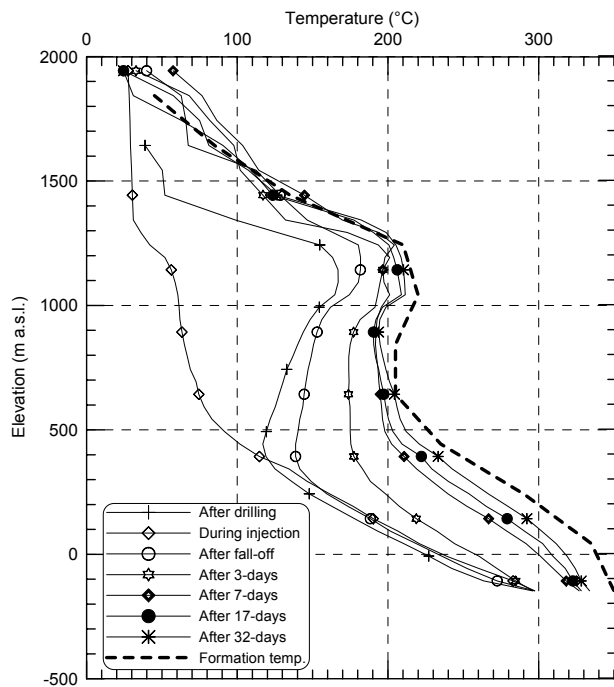


FIGURE 7: Temperature profiles in well OW-903

subsequent recovery profiles also indicate considerable rise in temperature in this region. This anomaly suggests the existence of a lateral reservoir flow in this zone. The temperature profiles are generally convective above 700 m a.s.l. and conductive below this depth. One would, therefore, expect permeability only above this depth.

aquifer in this range. The marked increase in the temperature gradient at 350 m a.s.l suggests that most permeable zones exist above this point. The temperature profile during injection indicates a slight gradient change between 750 and 650 m a.s.l., a distinct change at 650-600 m a.s.l. and a major one at 400 m a.s.l., suggesting the possible existence of permeable zones and fluid losses into the formation at these depths. The temperature profiles taken after fall-off indicate a kick at 1300 m a.s.l. This suggests that a hot feeder exists in this range. Note the almost constant 240°C temperature at 1000 to -300 m a.s.l. depth. This may be taken as a sign of vertical convection and a proximity to fracture permeability.

Well 903: Drilling was completed on 20th May 1999. The collected down-hole temperature data and estimated formation temperature are shown in Figure 7. The first log indicates a very sharp rise in temperature from 52°C at 1450 m a.s.l. to 167°C at 1200 m a.s.l. The injection and

4. ANALYSIS OF STATIC AND TRANSIENT PRESSURE DATA

4.1 Initial pressure conditions

The pressure logs obtained during completion tests and the recovery period for Olkaria Domes wells are shown in Figures 8, 9, and 10. It was observed that pressure profiles for all three wells pivot between 1100 and 900 m a.s.l. suggesting that the main productive reservoir is within that depth range. This is in accordance with the formation temperature analysis, which suggests productive reservoir with lateral flow at the same depth interval.

The calculated formation temperatures (Chapter 3) were substituted into the PREDYP program to estimate reservoir pressure. The program calculates pressure in a static water column, if the temperature of the column is known (Arason and Björnsson, 1994). Also required for the calculations is either the water level or the well-head pressure. Water level was adjusted in the

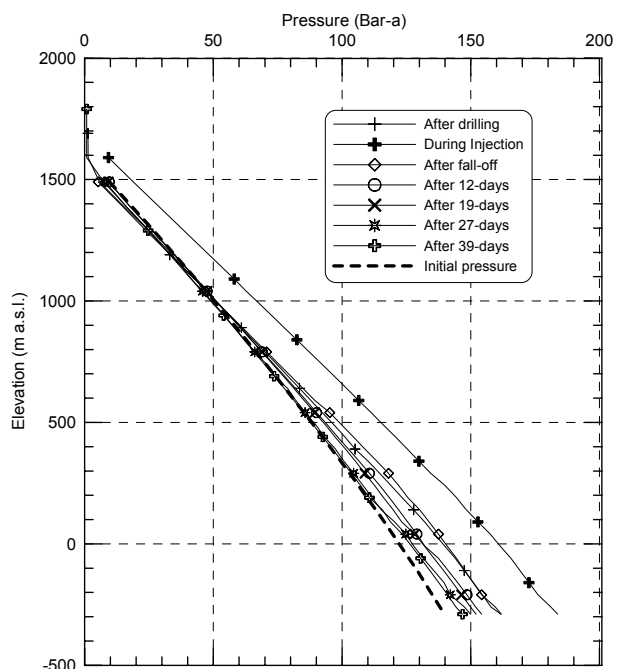


FIGURE 8: Pressure profiles in well OW-901

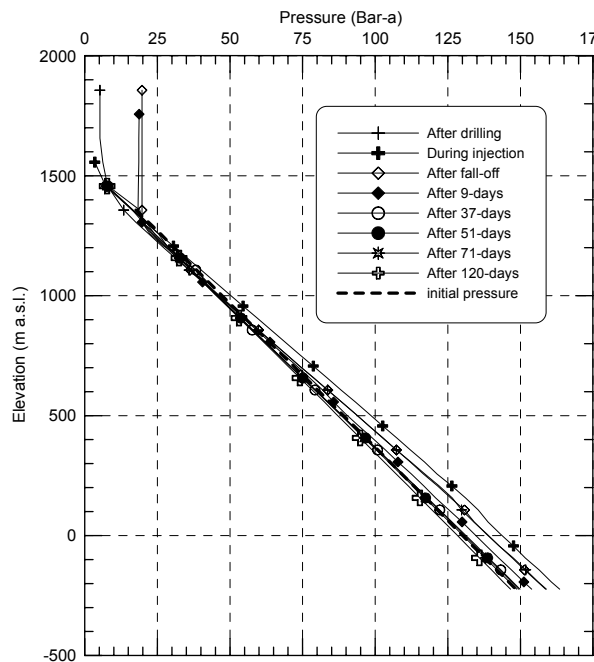


FIGURE 9: Pressure profiles in well OW-902

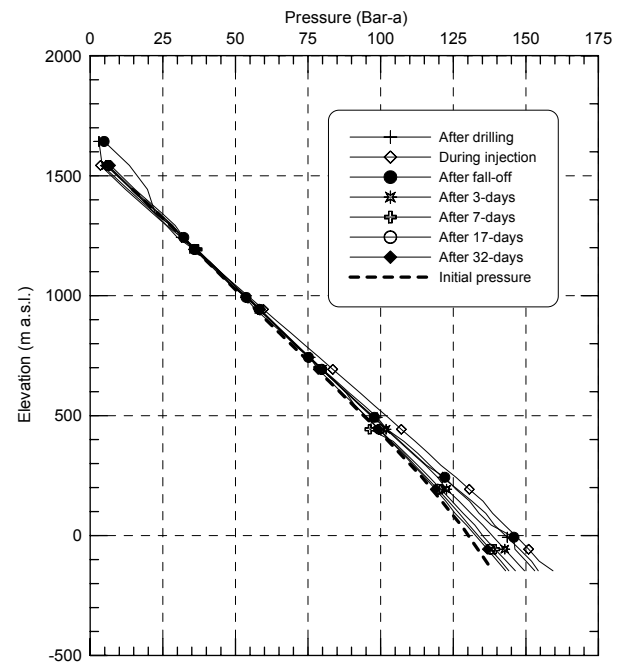


FIGURE 10: Pressure profiles in well OW-903

calculations until the calculated profile matched the pivot point pressure. This pressure match was achieved with water levels at 1600 m a.s.l. for OW-901, 1550 m a.s.l. for OW-902 and 1600 m a.s.l. for OW-903. The numerical values of the estimated initial pressure profiles and the formation temperatures are shown in Table 3.

TABLE 3: Estimated formation temperatures and initial pressures for the Olkaria Domes wells

OW-901			OW-902			OW-903		
Elevation (m a.s.l.)	Press (bar-a)	Temp. (°C)	Elevation (m a.s.l.)	Press (Bar-a)	Temp. (°C)	Elevation (m a.s.l.)	Press (bar-a)	Temp. (°C)
1690		140	1757		90	1843		45
1490	9.64	180	1557		100	1643		85
1290	26.73	215	1357	17.6	170	1443	14.56	135
1090	43.18	235	1257	26.15	217	1343	23.38	200
890	58.96	260	1157	34.39	225	1243	31.82	210
690	74.15	275	1057	42.57	228	1143	40.20	212
490	88.84	290	957	50.86	210	1043	48.51	220
290	102.97	305	757	67.68	210	843	65.27	205
90	116.45	320	557	84.39	220	643	82.22	205
-110	129.13	335	357	100.95	225	443	98.83	235
-290	139.75	345	157	117.35	235	243	114.25	290
			-43	133.58	240	43	127.71	335
			-223	148.45	240	-147	138.61	350

4.2 Pressure transient analysis

Injection or production causes pressure disturbance and by monitoring the response, parameters that control the reservoir and well behaviour can be evaluated. In the analysis, the following is usually carried out:

- Determination of average transmissivity, formation pressure and storage. These estimates are critical input into reservoir simulators and also for estimation of well productivity.

- Determination of skin effect to understand the nature of feed zones and to help decide if the well can be improved by stimulation.
- Determination of flow characteristics and the near well reservoir characteristics such as the influence of fractures, leaky boundaries, impermeable boundaries and, where possible, shape or size of the drainage area.
- Determination of optimum well test design.

Mathematical models have been developed that simulate the reservoir response to the flow rate history to estimate these parameters. The foundation for these models is the pressure diffusion equation. The pressure diffusion equation is written for radial flow as (Sigurdsson, 1999; Hjartarson, 1999):

$$\frac{1}{r} \frac{\partial}{\partial r} \left[r \frac{\partial P}{\partial r} \right] = \frac{\phi \mu c}{k} \frac{\partial P}{\partial t} \quad (2)$$

where P = Pressure;
 r = Radial distance from injection/production well and;
 t = Time.

It describes the isothermal flow of fluid in porous media where a well is producing or injecting at a constant rate and the medium porosity is denoted with ϕ , c is the reservoir compressibility, h is the reservoir thickness, k is the permeability and μ is the dynamic viscosity of water. It is the basic equation for well test analysis. A number of reservoir models are based on various solutions to this partial differential with different boundary solutions.

Some main assumptions in the derivation are

- The porous media is isotropic, homogeneous, horizontal of uniform thickness with constant porosity and permeability;
- A single-phase fluid is present and occupies the entire pore volume;
- The viscosity and compressibility of the fluid remains constant at all pressures;
- Pressure gradients are small, gravity forces negligible and a well completely penetrates the reservoir.

The equation of state relates pressure and density, for slightly compressible materials, the definition of isothermal compressibility c

$$c = \frac{1}{\rho} \left[\frac{\partial \rho}{\partial P} \right]_T \quad (3)$$

From this equation it can be shown that

$$\phi \frac{\partial \rho}{\partial t} = \phi c_f \rho \frac{\partial P}{\partial t} \quad (4)$$

and

$$\rho \frac{\partial \phi}{\partial t} = (1 - \phi) \rho c_r \frac{\partial P}{\partial t} \quad (5)$$

where c_f = Compressibility of the fluid;
 c_r = Compressibility of the rock.

This gives

$$\frac{\partial}{\partial t} (\phi \rho) = \rho c_t \frac{\partial P}{\partial t} \quad (6)$$

where c_t = Total compressibility of the system written as

$$c_i = \phi c_f + (1 - \phi) c_r \quad (7)$$

A special solution to the pressure diffusion equation (Equation 2) is the so called **Theis solution**. The appropriate initial and boundary conditions for the reservoir system are then

$$P(r,t) = P_i \quad \text{for } t=0, \quad r>0 \quad (8)$$

$$P(r,t) = P_i \quad \text{for } r \rightarrow \infty, \quad t>0 \quad (9)$$

$$q = \lim_{r \rightarrow 0} 2\pi \frac{kh}{\mu} \frac{\partial P}{\partial r} \quad t>0 \quad (10)$$

where q = Production / injection rate (kg/s).

The outer boundary condition, (9), describes constant pressure at infinity while the inner boundary condition, (10), is a flow condition through the well which has a radius close to zero (line source) in comparison to the infinite reservoir. The solution to the problem is the so-called *Theis solution*:

$$P(r,t) = P_i + \frac{q\mu}{4\pi kh} Ei\left(-\frac{\mu c_i r^2}{4kt}\right) \quad (11)$$

where Ei = The exponential integral function, defined as:

$$Ei(-x) = -\int_x^{\infty} \frac{e^{-u}}{u} du \quad (12)$$

This can be expanded as a Taylor series and substituted back into the *Theis solution* to yield

$$P(r,t) \approx P_i + \frac{2.303q\mu}{4\pi kh} \left[\log\left(-\frac{\mu c_i r^2}{4kt}\right) + \frac{\gamma}{2.303} \right] \quad (13)$$

where γ = The Euler constant = 0.5772.

The equation is found to hold accurately for $t \geq 100 \mu c_i r^2 / 4k$. It describes pressure draw-down at a distance r at time t when a well is producing/injecting at a constant rate q in a radial reservoir model.

4.3 Application to field data

By monitoring pressure changes with time in the field, it is possible to fit the observed pressure history to the theory and identify two important parameter groups: transmissivity (kh/μ) and storativity ($c_i h$). Permeability describes the medium's ability to transmit fluid while storativity describes its ability to store fluid. Equation 13 can be rearranged as $\Delta P = A + m \log t$. A plot of pressure change against time on a semi-logarithmic scale yields a straight line of slope m and constant A . Re-arranging terms, we have for the reservoir transmissivity (kh/μ):

$$\frac{kh}{\mu} = \frac{2.303q}{4\pi m} \quad (14)$$

If the reservoir temperature and hence viscosity μ is known, Equation 14 can be re-arranged to give the permeability thickness (kh). By using the draw down $\Delta P = P_i - P(r,t)$ at time t as a boundary condition in Equation 13 and rearranging, one gets storativity as:

$$c_t h = 2.25 \frac{kh}{\mu} \frac{1}{r_w^2} + 10^{-\Delta P/m} \tag{15}$$

In most well tests, the same well serves as a monitoring and production well. The radius in Equation 15 is simply the well radius r_w . Furthermore, by plotting ΔP as a function of the logarithm of time, one can extrapolate to find the time t_o when $\Delta P = 0$. By inserting into Equation 15, storativity is:

$$c_t h = 2.25 \frac{kh}{\mu} \frac{t_o}{r_w^2} \tag{16}$$

Note that the above formulae hold also for fall-off tests. In these, the time t is replaced with the Horner time τ (Equation 1) where time t is the total injection time before start of fall-off and Δt is the time elapsed during the tests.

4.4 Transmissivity and storativity for the Olkaria Domes

Analysis of transient pressure data from the Olkaria Domes was done in the following steps:

- Plotting pressure change during fall off against time or Horner time in a logarithmic scale (Figure 11);
- Calculating gradient (m) of straight portion of the graphs;
- Identifying time (t_o) on the straight portion when $\Delta P = 0$; and
- Substituting for these parameters in Equations 14 and 16 to estimate well transmissivity, storativity and permeability based on an average reservoir thickness of 500 m and hot reservoir (200°C) dynamic viscosity of 1.3×10^{-4} kg/m/s.

The results are presented in Table 4. Note that only permeabilities based on fall-off data are shown, as the build up pressure tests were too distorted for this simple analysis. Figure 12 shows this in more detail.

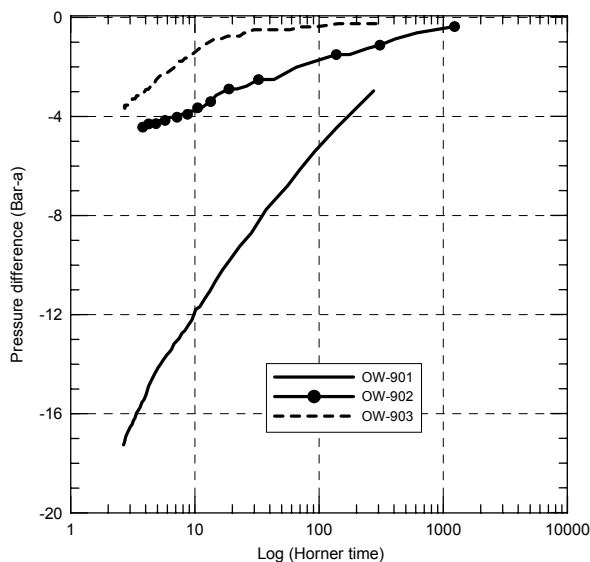


FIGURE 11: Pressure fall-off profiles in wells OW-901, OW-902 and OW-903

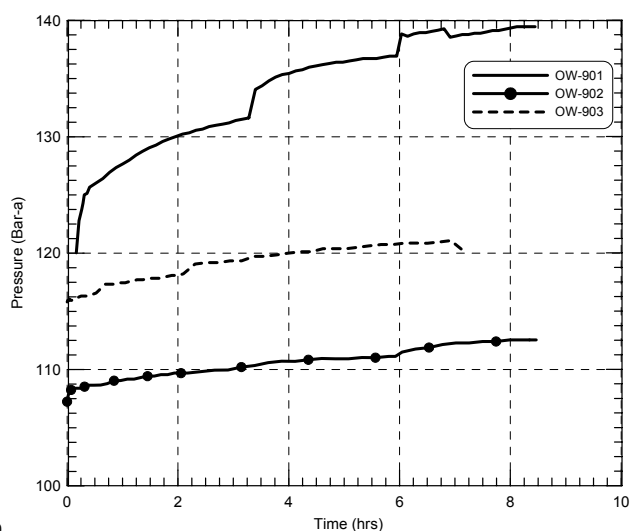


FIGURE 12: Injection tests in Olkaria Domes

With the exception of well OW-902, the figures obtained are much lower than the Olkaria field average steam zone permeability of 7.5 mD and liquid zone permeability of 4.0 mD (Merz and McLellan, 1984).

TABLE 4: Transmissivities, storativities and injectivities in the Domes wells

Well number	Fall-off Horner gradient	Horner time at $\Delta P=0$ (s)	Transmissivity ($m^3/Pa.s$)	Permeability thickness (D-m)	Permeability (mD)	Storativity (m/Pa)	Injectivity (lps/bar)
OW-901	112000	486	0.44×10^{-8}	0.436	0.9	4.8×10^{-4}	1.23
OW-902	16000	18	3.05×10^{-8}	3.054	6.1	1.2×10^{-4}	3.92
OW-903	40000	2160	1.22×10^{-8}	1.221	2.4	59.4×10^{-4}	6.20

4.5 Injectivity

Down-hole pressures did not stabilise during the time allocated for injection tests in the Domes (Figure 12). However, the last pressure values for each flow step can be plotted against the rates and best-fit lines drawn. Figure 13 is an example of such a plot for well OW-902. The slope of such lines then yields injectivity of the wells. The injectivity results are included in Table 4.

5. A CONCEPTUAL RESERVOIR MODEL

A carefully developed conceptual reservoir model serves as a cornerstone in the classification and operation of a geothermal field. Among key figures in such models are the formation temperatures and initial pressures of the respective wells. Here a two-step approach is used to present the conceptual model. Firstly a local Domes model is presented, based on the previous data analysis in wells 901-903. Secondly, the Domes model is included in the greater Olkaria conceptual model to better understand the basic heat and mass flow within the Olkaria caldera.

5.1 The Domes

Figure 14 shows formation temperatures for OW-901, OW-902 and OW-903. The graph indicates near uniform temperature in all the wells in a zone immediately above 1000 m a.s.l. We can therefore suggest that in the Olkaria Domes field, a homogeneous horizontal layer exist just above 1000 m a.s.l.

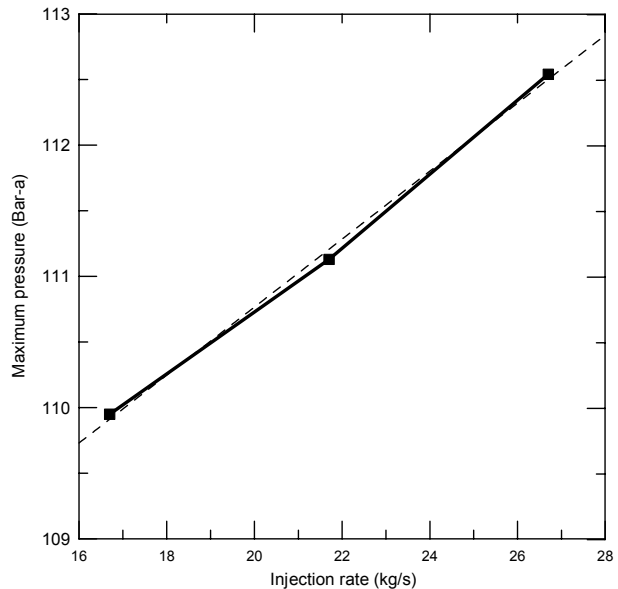


FIGURE 13: Injectivity of well OW-902

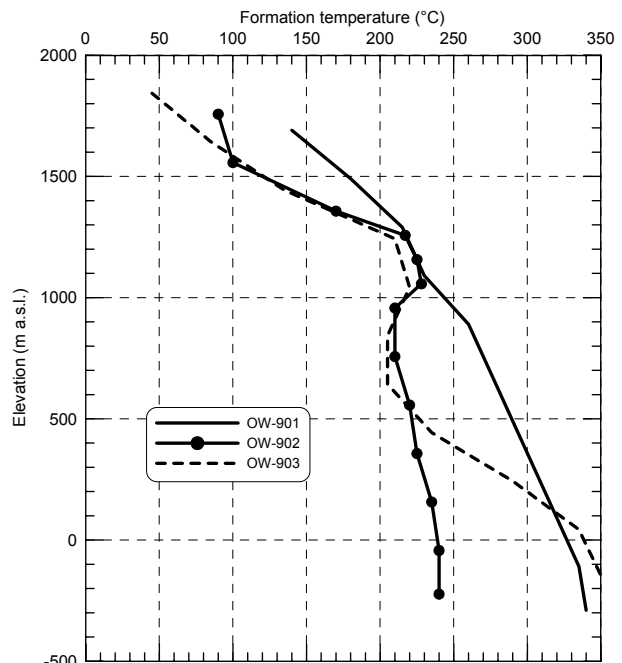


FIGURE 14: Estimated formation temperatures in Olkaria Domes

Considering individual well profiles, it is observed that OW-901 exhibits a conductive profile, suggesting a possible lack of permeability. This is unlike OW-902 which exhibits near uniform temperature between 1200 m a.s.l. and the bottom. This well may be drilled in the vicinity of good vertical permeability. It is also worth noting that the 240°C bottom-hole temperature of OW-902 is the coldest in Olkaria Domes. These results show that these three wells have different characteristics, but with a common feature, the permeable horizontal layer above 1000 m a.s.l.

Figure 15 is a plot of temperature profiles during injection for the three wells. Although the wells are scattered within the field, the profiles exhibit a striking similarity. All the wells have increased temperatures below 400 m a.s.l. The logs run actually side by side for the most part in wells OW-901 and OW-902. Of particular interest are steps which occur in the temperature profiles at practically the same elevations in all three wells. These are due to water loss into the formation and, hence, a more rapid heating of the wellbore fluid below the feedzones. This suggests that permeability in the Domes is dominated by the same three horizontal structures.

The estimated reservoir pressures for wells 901-903 are plotted together in Figure 16. The highest pressure is found in well OW-903 and lowest in the upper zone of OW-902. This is the same zone identified by the temperature logs and formation temperatures as the productive reservoir. Note that this analysis is unreliable for the deeper sections of the wells as they are practically impermeable in that region.

In summary, the following can be stated as a conceptual model for the Olkaria Domes:

- The field has adequate horizontal permeability with the main reservoir existing in a layer just above 1000 m a.s.l. containing hot water with temperatures ranging from 210-230°C (Figures 14 and 15).
- OW-901 is drilled in a location of low permeability. It is, therefore, a good indicator of the thermal gradient in the field. The mean value is 150°C, but it is higher at shallow depths and lower at greater depths.
- Good permeability in OW-902 is a possible indication of it being located within or near a vertical fault zone. The low pressure is an indication of natural drainage of the field to the south.
- The reservoir pressure reduces southwards and westwards.

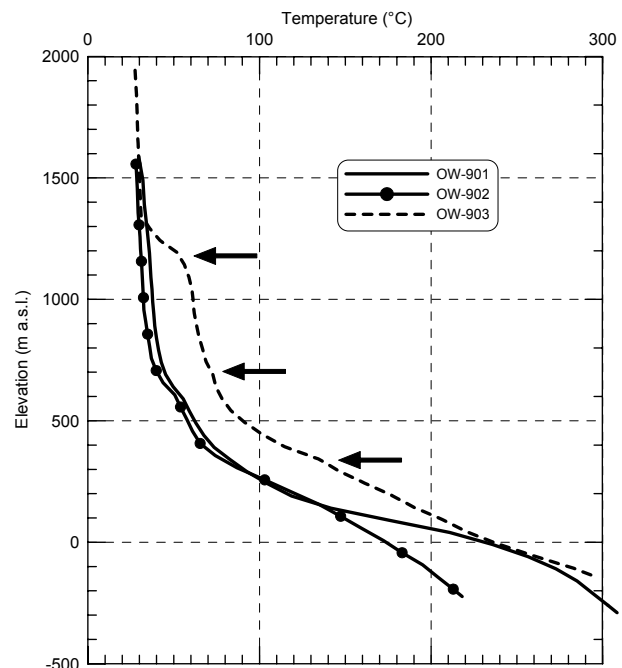


FIGURE 15: Temperature profiles during injection in the Olkaria Domes, location of major feed-zones is shown by arrows

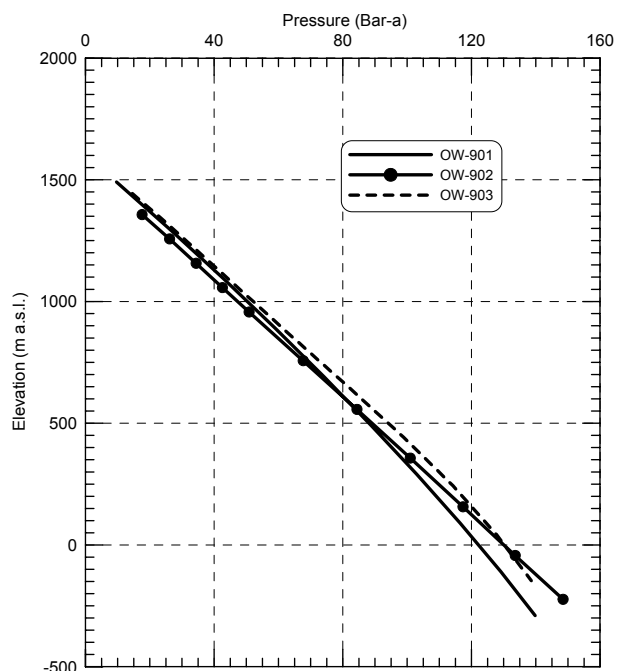


FIGURE 16: Formation pressure profiles for Olkaria Domes

6. RESOURCE ASSESSMENT

A preliminary resource assessment is usually done upon completion of surface mapping, drilling and testing in a new geothermal field. Ideally, the results of such studies should indicate whether development drilling could go on and, if so, should identify probable targets for future wells. The study also includes an initial estimate of the capacity of the field. An update of this study could be prepared as more wells are drilled and tested and put into production.

Three methods are usually applied in the estimation of a potential reserve:

1. Volumetric method for calculation of stored heat, when no production history is available;
2. Lumped parameter models;
3. Distributed parameter model or numerical simulation.

Here, the volumetric method is applied to the three wells in the Domes which were drilled to completion, and tested as described in the previous chapters. This type of analysis should, however, be taken as preliminary and replaced by numerical modeling as more field data becomes available.

6.1 Volumetric production capacity

The volumetric method is used in calculating the amount of energy that *might* be recoverable from a reservoir (Amdeberhan, 1998). It involves substitution of probable quantities in definite equations making reasonable assumptions to determine probable results. The basic principle is that the total energy recoverable from a geothermal system is the sum of energy recoverable from rock and a component recoverable from water. The thermal energy in the subsurface is calculated from the equation:

$$E = E_r + E_w = VC_r \rho_r (1 - \phi)(T_i - T_o) + VC_w \rho_w \phi (T_i - T_o) \quad (17)$$

where E = Total thermal energy in the rock, r , and water, w [J];
 V = Volume of reservoir [m^3];
 T_i = Initial reservoir temperature [$^{\circ}C$];
 T_o = Reference temperature [$^{\circ}C$];
 $C_{r,w}$ = Heat capacity of rock, water [$J/kg^{\circ}C$];
 $\rho_{r,w}$ = Density of rock, water [kg/m^3];
 ϕ = Porosity.

The relationship below then calculates the electrical power potential of a reservoir:

$$Reserve(MWe) = \frac{\text{heat energy} \times \text{recovery factor} \times \text{conversion efficiency}}{\text{plant life} \times \text{load factor}} \quad (18)$$

Based on the temperature profiles and physical boundaries of the area (Figures 17 and 18), the following assumptions can be made for the Olkaria Domes reservoir as the most likely:

$$\begin{array}{llll} T_o = 200^{\circ}C & C_r = 1000 \text{ J/kg}^{\circ}C & C_w = 4200 \text{ J/kg}^{\circ}C & T_i = 225^{\circ}C \\ \phi = 5\%, & \rho_r = 2700 \text{ kg/m}^3, & \rho_w = 840 \text{ kg/m}^3, & \text{Reservoir area} = 4 \text{ km}^2 \\ \text{Reservoir thickness} = 500 \text{ m} & & & \end{array}$$

Inserting these values in Equation 17 results in an estimate of 1.37×10^{17} J of stored heat energy. Assuming a recovery factor of 0.2, turbine conversion efficiency of 0.1, load factor of 0.95 and plant life of 30 years. Substituting this into Equation 18 gives an electric power for the Olkaria Domes reservoir as **3 MWe**.

6.2 The Monte Carlo probability method

This involves substitution of probable quantities in definite equations making reasonable assumptions to determine the most probable results (Samiento, 1993). The basic equations remain 17 and 18 above, but recognition is made of the fact that many parameters in the subsurface cannot be defined with certainty. They are, therefore, considered to have some uncertain values between carefully predetermined constants. Here, the following assumptions are made:

- T_i varies between 210°C and 250°C,
- Porosity (ϕ) varies between 2 and 8%,
- Density (ρ_r) of the reservoir rock varies between 2400 and 3000 kg/m³,
- Density (ρ_w) of water varies between 800 and 850 kg/m³,
- Reservoir area varies between 3 and 5 km², and
- Reservoir thickness varies between 300 and 700 m.

Random number generation is used to solve the algorithm relating to these uncertainty distributions by randomly assessing the values from each distribution individually many times. This results in a probability distribution for the reserve estimate that quantitatively incorporates the uncertainties involved in each parameter. The randomness of certain values is defined here either by square or triangular method. Generally, a square distribution is used when any value within a definable limit is considered a possibility. A triangular method is used when the best guess value for a parameter (most likely nodal value) is possible along high and low extremes.

The square probability method is applied here to the reservoir area, thickness, initial temperature and water density, while rock density and porosity are assigned triangular random values. All the remaining factors are treated as constants within the reservoir. Table 5 summarizes this.

TABLE 5: Best guess and probability distribution for the Monte Carlo analysis

Property	Unit	Best guess model	Probability distribution		
			Type	From	To
Area	km ²	4	square	3	5
Reservoir thickness	m	500	square	300	700
Rock density	kg/m ³	2700	triangle	2400	3000
Rock specific heat	J/kg°C	1000	constant		
Porosity	%	5	triangle	2	8
Reservoir temperature	°C	225	square	250	210
Reference temperature	°C	200	constant		
Water density at reservoir temp.	kg/m ³	833.9	square	800	850
Water specific heat at reservoir temp.	J/kg°C	4200	constant		
Recovery factor for reservoir	%	0.2	constant		
Thermal efficiency for turbine	%	0.1	constant		
Plant load factor	%	0.95	constant		
Plant life period	Year	30 years	constant		

After assigning various random values and constants, the rest of the calculation was accomplished in the following fashion:

1. A matrix of 8 × 1000 was created on an Excel spreadsheet, each column in the matrix containing random numbers. The random numbers were generated using Excel function RAND which produces numbers between 0 and 1.
2. Formulae were put in additional columns to transform the random numbers into the desired range for

various quantities. As an example, a square distribution of reservoir area was calculated as:

$$A = 3 \times 10^6 + RI \times (5-3) \times 10^6$$

where *RI* is a random number generated. For a triangular distribution for reservoir porosity, the mean of two random numbers *R3* and *R4* is used thus:

$$\phi = 2 + ((R3 + R4) / 2) \times (8-2)$$

where again a minimum of 2% and maximum of 8% porosity are assumed.

3. Equations 17 and 18 were put into additional columns to calculate energy reserve and electric power potential.
4. The estimated power production capacity was then plotted as a histogram (Figure 20).

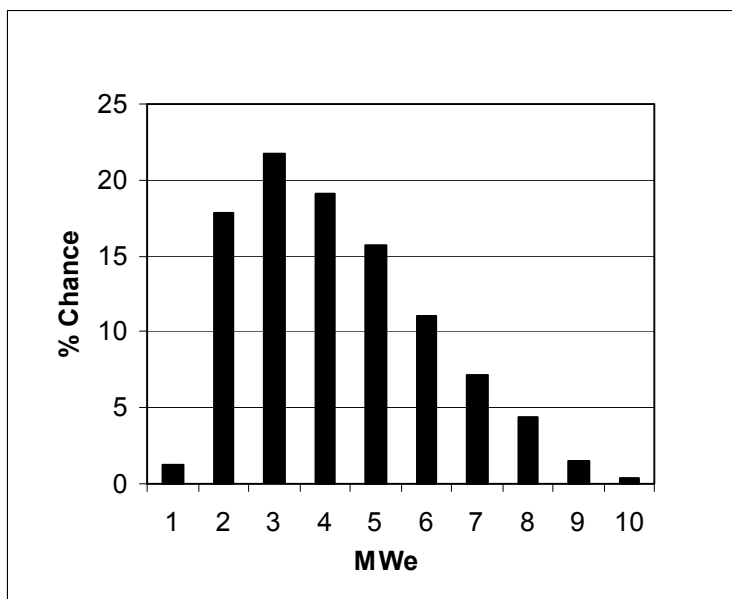


FIGURE 20: Frequency distribution of available electric power in Olkaria Domes

The histogram indicates that the range of probability estimate is from 0 to 10 MWe. The most likely value is in the range 2-5 MWe. A cumulative frequency curve shows that the most likely value of the reserve (median) is 3.5 MWe, and that there is less than 20% chance of the reserve being more than 5 MWe or less than 2 MWe.

It is also important to point out at this stage that 2.2 kg/s of high-pressure steam generally are required to produce 1 MWe. Unfortunately, none of the present Domes wells can produce high-pressure steam (Table 2). This fact is not included in the Monte Carlo analysis. We are, therefore, not able to make a conclusion on the number of wells required in Olkaria Domes to obtain the 3.5 MWe mean capacity.

7. FEASIBILITY OF RE-INJECTION

The previous work shows that three wells drilled into Olkaria Domes have low production capacity, permeability and energy reserve. Additional power plant development should, therefore, be regarded as unfeasible unless permeable formations are discovered in areas of substantially higher temperature than the present horizontal reservoir. However, considerable funds have been committed to this field and one way of utilizing it would be through re-injection. In Were (1998), re-injection is proposed as one of the best ways of disposing of potentially pollutant effluent from the producing fields in Olkaria.

The following are some calculations carried out to determine possible cooling effects in the Olkaria East production field due to re-injection in Domes. To estimate this with reasonable accuracy, we have applied three simple reservoir models which predict the thermal efficiency of the re-injection.

In the first scenario (Axelsson, 1999), we assume that the medium transmitting fluid is a porous horizontal layer of constant thickness *h* (radial model). The time *t* taken for the injected fluid to reach out to a radius *r* is given by

$$t = \frac{\pi h \langle \rho \beta \rangle r^2}{\beta_w Q} \quad (19)$$

where $\langle \rho \beta \rangle$ = Average volumetric heat capacity of the reservoir rocks;
 β_w = Heat capacity of water; and
 Q = Injection rate.

Note that this model assumes no conductive heat flow.

In the second scenario, we assume that a narrow horizontal fracture transmits the injectate radially out. Here heat is transported by horizontal fluid convection in the fracture and by vertical conduction in the adjacent rocks. To determine the time when temperature at radius r is half way between the original reservoir temperature and injected fluid temperature, we use the following equation (Axelsson, 1999):

$$t = \left[\frac{2\pi K r^2}{\beta_w Q} \right]^2 \frac{1}{a_T} \quad (20)$$

where K = Thermal conductivity of the reservoir rocks; and
 a_T = $K/\rho\beta$ = Thermal diffusivity of the rocks.

Basically, Equations 19 and 20 only provide an estimate for the time passed until the injected fluid adversely cools a reservoir at a distance r from an injection well. We have substituted the following values for calculation into the equations:

- Specific heat capacity of water, $\beta_w = 4185 \text{ J/kg } ^\circ\text{C}$;
- Density of rock, $\rho = 2750 \text{ kg/m}^3$;
- Specific heat capacity of rock, $\beta = 1000 \text{ J/kg } ^\circ\text{C}$;
- Thermal conductivity of rock, $K = 2 \text{ W/m } ^\circ\text{C}$;
- Reservoir thickness, $h = 500 \text{ m}$;
- Mean distance between the Domes and the East production field, $r = 2000 \text{ m}$

Thus, if the initial temperature of the reservoir is denoted by T_o , the temperature of the reservoir during injection by T_r , and temperature of the injected fluid by T_i , then we have results as shown in Table 6.

TABLE 6: Estimated cooling times for Olkaria East production field due to re-injection in the Domes

Injection rate (kg/s)	Porous Model	Fracture Model
	Time (yr) when $T_r = T_i$	Time (yr) when $T_r = (T_i + T_o)/2$
25	5200	10000
30	4400	7000
40	3300	3900
50	2600	2500
75	1750	1100
100	1300	600

The presence of a horizontal permeable layer in the conceptual reservoir model means that the models described in Equations 19 and 20 are reasonable. These calculations suggest that there is little risk of cooling the East production field during the economic life of the power generating plant.

In the two radial models presented above, only a fraction of the injected fluid shows up in the East production field. The third and the worst case scenario is application of a reservoir model TRCOOL (Axelsson et al., 1994) to calculate what may be defined as extremely fast thermal break-through time.

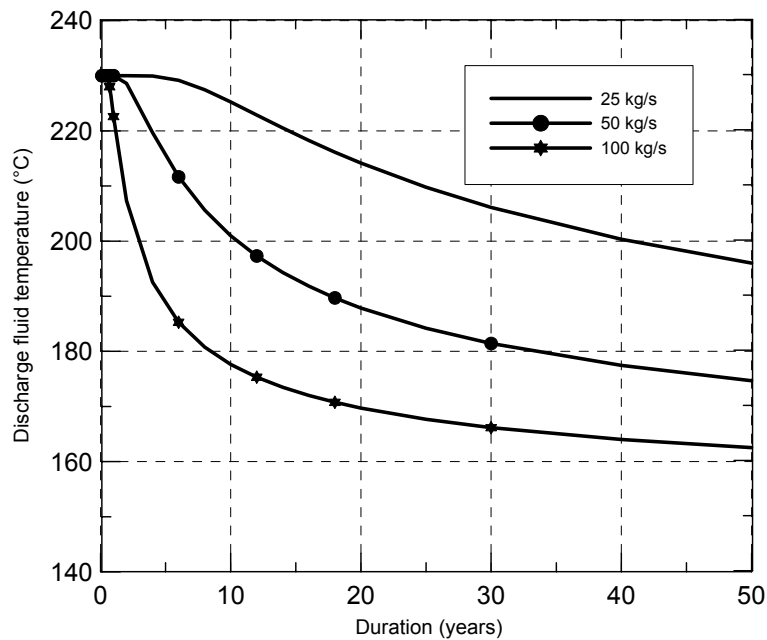


FIGURE 21: Outlet temperatures for a thin rectangular flow channel connecting the Olkaria East field and the Domes

calculated by the TRCOOL software.

Inspection of Figure 21 shows that for the case of 25 kg/s injected, based on this very pessimistic reservoir model, it will take more than 25 years for the discharge to cool below 200°C in the East production field. Higher injection rates may, however, cause serious cooling. As temperatures during injection suggest that more than one horizontal layer connects the Domes and the East production field (Figure 16), it is considered likely that the injectate will be divided between several flow channels. This means that adverse cooling in the East production field is also considered unlikely in this model, as in the other two.

Finally, it should be noted that pressure decreases rapidly to the south in Olkaria and that the Domes appear to be downstream when compared to the other Olkaria well fields. It is, therefore, likely that a sizeable fraction of fluid injected in the Domes will flow to the south and out of the reservoir.

8. CONCLUSIONS

In this study, results of tests done in wells OW-901, OW-902 and OW-903 in Olkaria Domes were analysed. The tests included down-hole temperature and pressure profiles, injection tests, fall-off tests and discharge tests. Injection and fall-off tests were used to calculate permeability, transmissivity and storativity.

Results of discharge tests show that the Domes wells have low production capacity, and injection tests show that with the exception of well OW-902, permeability of these wells is much lower than the Olkaria field average of 7.5 mD for steam zone and of 4.0 mD for liquid zone.

Formation temperature and pressure were defined by applying programs BERGHITI and PREDYP to the down-hole data. Together with the injection profiles, these were input into the conceptual model which suggests that permeability in the Domes is confined to a horizontal layer above 1000 m a.s.l. It further suggests that the greater Olkaria system drains naturally southwards. High bottom-hole temperature in wells OW-901 and OW-903 suggests the existence of a hot intrusive body in the Domes, but the main

The model assumes that a thin fracture zone (flow channel) connects a re-injection and a production well and that all the injected fluid flows to the producer. The flow channel is assumed to be of constant height/width h , constant thickness b such that $b \ll h$ and porosity ϕ . As in the case of Equation 19, the fracture model considers only convective heat flow in the fracture and only conductive in the adjacent rocks. We have assumed a mean initial reservoir temperature between the Domes and the East production field to be 230°C, temperature of injected water to be 150°C, fracture width to be 500 m and that injection rate is equal to production rate. Figure 21 is a plot of the flow channel output temperature against time as

reservoir at 1000 m a.s.l. has low temperature and low permeabilities resulting in low productivity. Volumetric and Monte Carlo analysis show that the energy reserve in Domes is between 2 and 5 MWe but exploitation of this is only possible if higher permeabilities are found.

A feasibility study of re-injection into the Domes field was done especially to predict the rate of cooling in the East production field reservoir. It showed that for radial, horizontal models, and while injecting at 100 kg/s, it would take more than 100 years before some minor cooling takes place in the East production field. For a one-dimensional fracture model, which is the worst case, more than one flow channel is needed to secure a successful injection rate of 100 kg/s for tens of years. It is, therefore, recommended that one possible way for utilizing the investment made in the Domes, is by long term re-injection.

ACKNOWLEDGEMENTS

I would like to thank Dr. Ingvar B. Fridleifsson, Lúdvík S. Georgsson and Gudrún Bjarnadóttir of United Nations University, Geothermal Training Programme for giving me the chance to participate in the training programme and for their support during my training and living in Iceland. I am very grateful to the government of Iceland for its role in funding this programme and to all the staff at Orkustofnun for their invaluable lectures and professional advice. I would like to thank the reservoir engineers Benni, Gudni and Ómar for their role in my training and to Steinar for his direction of this project. I am most grateful to Grímur Björnsson for his direct involvement in the supervision of this work. Despite his busy schedule, he was always available to criticise this work and to share his experience and knowledge.

I would like to thank the Kenya Electricity Generating Company for allowing me the sabbatical leave to do this course, and especially to Cornel Ofwona who always sent data and information whenever I requested it. Many thanks to my family, Jane, Max and Sam for their moral support and for enduring my long absence from home.

REFERENCES

- Amdeberhan, Y., 1998: A conceptual reservoir model and production capacity estimate for the Tendaho geothermal field, Ethiopia. Report 1 in: *Geothermal training in Iceland 1998*. UNU G.T.P., Iceland, 1-24.
- Arason, P., and Björnsson, G., 1994: *ICEBOX*, 2nd edition, Orkustofnun, Reykjavík, 38 pp.
- Axelsson, G., 1999: *Fundamentals of geothermal reservoir physics*. UNU G.T.P., Iceland, unpublished lecture notes.
- Axelsson, G., Björnsson, G., and Arason, P., 1994: *TRCOOL program*. Orkustofnun, Reykjavík.
- Bödvarson, G.S., Pruess K, Haukwa C and Ojiambo S B, 1989: Evaluation of reservoir model predictions for the Olkaria East geothermal field, Kenya. *Proceedings of the 14th Workshop on Geothermal Reservoir Engineering, Stanford University, CA*, 95-104.
- Bödvarson, G.S., Pruess K., Stefánson V., Björnsson S., Ojiambo S.B., 1987: East Olkaria Geothermal field, Kenya – History match with production and pressure decline data. *J. Geophys. Res.*, 92-B1, 521-539.
- Haukwa, C.B., 1985: *Analysis of well test data in the Olkaria West geothermal field, Kenya*. UNU

G.T.P., Iceland, report 5, 76 pp.

Helgason, P., 1993: *Step by step guide to BERGHITI. User's guide.* Orkustofnun, Reykjavík, 17 pp.

Hjartarson, A., 1999: *Analysis of reservoir data collected during re-injection into the Laugaland geothermal system in Eyjafjörður, N-Iceland.* M.Sc. thesis, University of Iceland and Orkustofnun.

Lagat, J., 1995: Borehole geology and hydrothermal alteration of well OW-30, Olkaria Geothermal Field, Kenya. Report 6 in: *Geothermal Training in Iceland 1995*, UNU G.T.P., Iceland, 135-154.

Merz & McLellan-Virkir, 1984: *Status report on steam production.* The Kenya Power Company Ltd., Olkaria Geothermal Project, report.

Muna, Z.W., 1997: *Conceptualized model of Greater Olkaria geothermal field.* Kenya Power Company, internal report, 20 pp+figs.

Sarmiento, Z.F., 1993: *Geothermal development in the Philippines.* UNU G.T.P., Iceland, report 2, 99 pp.

Sigurdsson, Ó., 1999: *Basic well test theory.* UNU G.T.P., Iceland, unpublished lecture notes.

Were, J.O., 1998: Aspects of waste management and pollution control in Olkaria geothermal field, Kenya. Report 16 in: *Geothermal Training in Iceland 1998*, UNU G.T.P., Iceland, 423-460.